Bioelectrochemistry 133 (2020) 107488

Contents lists available at ScienceDirect

Bioelectrochemistry

journal homepage: www.elsevier.com/locate/bioelechem

Rapid detection of biodegradable organic matter in polluted water with microbial fuel cell sensor: Method of partial coulombic yield

Yangyang Gao [a,b,c], Fengjun Yin [a,b,c], Weiqi Ma [a,b,c], Sha Wang [a,b,c], Yuan Liu [a,b,c], Hong Liu [a,b,c,*]

[a] Key Laboratory of Reservoir Aquatic Environment, Chinese Academy of Sciences, Chongqing 400714, China
[b] Chongqing Institute of Green and Intelligent Technology, Chinese Academy of Sciences, Chongqing 400714, China
[c] University of Chinese Academy of Sciences, 100049 Beijing, China

ARTICLE INFO

Article history:
Received 28 September 2019
Received in revised form 15 February 2020
Accepted 15 February 2020
Available online 24 February 2020

Keywords:
Biodegradable organic matter
Partial coulombic yield
Cutoff point
Biosensor

ABSTRACT

The quantification of biodegradable organic matter (BOM) in polluted water plays an essential role for biodegradation-based processing of wastewater and management of water environment. Compared with the traditional detection of five-day biochemical oxygen demand (BOD_5), microbial fuel cell (MFC) sensors have shown an advantage for rapid and more accurate BOM assessment in several hours using coulombic yield of MFC as the signal. In this study, we propose a new calculation method that relies on the partial coulombic yield (P-CY) to further shorten the duration of the measurement. The P-CY is the cumulative coulomb at the point at which the voltage acquisition reaches a maximum voltage drop rate. The detection results with the standard GGA solution (a mixture of glucose and glutamic acid) show an enhanced linear relationship ranging from 37.5 mg L^{-1} to 375 mg L^{-1} in comparison to conventional methods. Notably, the response time for P-CY is remarkably shortened (0.99 ± 0.18–18.08 ± 0.58 h). The cutoff point for P-CY has more stable electrochemical characteristics, which enhances the accuracy of BOM detection. Furthermore, the validity of our determination of the cutoff point for P-CY is demonstrated by a mathematical model based on the Michaelis-Menten equation. Thus, the P-CY method is viable for the rapid detection of BOM in polluted water.

1. Introduction

Biodegradable organic matter (BOM) is such that it can be utilized by microorganisms to produce small molecules, including CO_2, H_2O, etc. Knowledge of the BOM value in polluted water is essential for the selection of water treatment processes, water quality management and assessment, ecology and environmental science [1]. The five-day biochemical oxygen demand (BOD_5) has been long employed as a proxy for BOM amount, but the associated testing method severely suffers from a longer response time, lower detection precision and higher requirement of manual labor and skills [2]. Optimized methods, such as oxygen probe and manometric methods, have emerged to improve the detection precision. Nevertheless, the required time has not reduced thus these methods failed to perform high-throughput analyses [2,3]. To shorten the measurement time, biosensors including bioluminescent bacteria, membrane electrode and bioreactor technology were successfully developed, but challenges remain in analyzing diverse samples and controlling costs [2,4,5].

Microbial fuel cell (MFC), as a novel bioelectrochemical system (BES), can be applied not only in energy recovery but also in wastewater treatment. In recent years, considerable attention has been paid to the application of MFCs as sensors in water quality monitoring. In the MFC matrix, a variation of target substrate affects the electron transfer processes initiated by the microorganisms, and thus brings changes in the electrical signals that can be quantified accurately. MFCs have been studied as biosensors for BOM, heavy metals, dissolved oxygen (DO), nitrates, volatile fatty acids (VFAs), etc. [6–8]. Compared to conventional biosensors, MFC sensors have advantages in self-sustainability and simplicity of operation.

There are three main approaches in analyzing electrical signals. The maximum current output of an MFC sensor is commonly used as the analytical signal. Hsieh et al. [9] constructed a dual-chamber MFC as a biosensor for BOD, where a good correlation between the peak current and BOD concentration of artificial wastewater was obtained. Second, the maximum open circuit voltage (OCV) has also been used for water quality monitoring. Wang at al. [10] employed an OCV to operate a MFC sensor (O-MFC sensor) for real-time nitrate monitoring, and it turned out that the O-MFC sensor was much more stable and sensitive when affected by organic

* Corresponding author.
E-mail address: liuhong@cigit.ac.cn (H. Liu).

https://doi.org/10.1016/j.bioelechem.2020.107488
1567-5394/

matter (NaAc). Third, the coulombic yield (CY) is also related to the concentration of the target analyte, and can be employed as the signal for BOD testing. Kim at al. [11] established a linear correlation between the CY and the BOD_5 of synthetic wastewater, such measurement system was successfully operated for over 60 days.

These approaches generally established a good relationship between the electrical signal and target analyte, yet drawbacks still exist. The maximum current output is susceptible to interference, restricting its use to a small detection range. At high substrate concentration, the maximum current output becomes saturated, give rise to signal distortion. For OCV, there is still uncertainty about the correlation between the water quality index and OCV, and MFC sensors cannot work in an open circuit for a long time [12]. These drawbacks hinder the application of OCV. The CY can be influenced by the unstable coulomb efficiency (CE) and ambiguous tail stage. The CE is an important indicator for measuring the conversion efficiency from organic substrates to electrons, which is affected by the dynamic competition between electrogens and nonelectrogens. Endogenous respiration can provide extra electrons at the tail stage, which impacts the accuracy of the CY [13].

In our previous study, a new index (BOM_Q) has been proposed to quantify BOM through the CY. The principle is that the quantity of generated electrons exhibits a one-to-one correspondence with the amount of BOM in anode and oxygen consumption in air cathode. This method is free of any calibration curve, and is effective for rapid and precise determination of BOM [1]. Based on this previous work, this research investigated partial coulombic yield (P-CY) as a novel method of calculating BOM concentration. The point of maximum voltage drop rate ($Max|\Delta Q/\Delta t|$) was regarded as the cutoff point for voltage acquisition. The corresponding index (BOM'_Q) can be calculated by P-CY. This method can avoid ambiguous tail stage of the voltage acquisition, and decrease response time. This approach evaluated the accuracy and sensitivity of MFC sensors to BOM, as well as the response time and stability. In addition to electrochemical analyses, a mathematical model was also established to validate the optimum cutoff point for the P-CY.

2. Materials and methods

2.1. MFC sensor construction and startup

A dual-chamber, cubic-shaped MFC was constructed as a biosensor, as previously described [1]. The anode and air–cathode chamber had a cylindrical interior and were separated by a proton exchange membrane (Nafion117, DuPont, USA). The anode chamber was 1 cm long and 3 cm in diameter, the air–cathode chamber was 2 cm long and 3 cm in diameter. A $\pi \times (1.5\ cm)^2$ piece of carbon cloth (W0s1009, Phychemi Co. Ltd., China) was used as the anode. A piece of carbon cloth (W1s1009, Phychemi Co. Ltd., China) was used as the air–cathode and contained poly (dimethylsiloxane) as a diffusion layer and Pt/C as the catalyst. The anode and cathode were connected through a resistor of 1000 Ω to record voltage. Before construction of the MFC, the anode carbon cloth was inoculated with abundant biofilm in the long-term stable large-scale MFC for over one month.

During start-up, each liter of anolyte contained 0.15 g glucose, 0.15 g glutamic acid, 0.13 g KCl, 0.31 g NH4Cl, 6.08 g NaH2PO4··2H2O and 21.83 g Na2HPO4··12H2O (0.1 M PBS), 12.5 mL trace minerals solution and 5 mL vitamins solution. Each liter of catholyte contained 6.08 g NaH2PO4··2H2O and 21.83 g Na2HPO4··12H2O [1]. The anolyte was bubbled with N_2 to remove dissolved oxygen before use. The medium of the MFC was replaced when the voltage decrease was<1 mV h^{-1}, and the MFC was operated at a constant temperature (30 °C) in an incubator. The startup of the MFC was successful when the CY of two consecutive cycles remained stable. The output voltage was recorded at a sampling interval of 5 min using a signal acquisition system (PCI-1747U, Advantech, China).

2.2. Quantification of BOM detection

After start-up, BOM can be detected by the MFC sensor. Before testing, the anode chamber was rinsed with 0.1 M PBS solution to empty existing electrolytes. In the testing stage, the anode chamber was filled with the sample solution and the cathode chamber was filled with 0.1 M PBS solution. The effective volume of the water sample was calculated by mass changes before and after sample injection. The voltage changes were recorded and the corresponding BOM values (BOM_Q) were calculated according to previous studies [1]. The standard GGA solution (the same amounts of glucose and glutamic acid) was selected as the model BOM. Experiments using different GGA concentrations (3.75, 7.5, 15, 37.5, 75, 150, 225 and 375 mg L^{-1}) were carried out, which corresponded to different theoretical BOD_5 values (5, 10, 20, 50, 100, 200, 300 and 500 mg L^{-1}). In addition, the real wastewater samples were pretreated by PBS to obtain an appropriate organic matter load and conductivity. The initial DO concentration of the water sample was maintained below 0.1 mg L^{-1}. Each sample was measured three times in parallel. An illustration of BOM detection by the MFC sensor is shown in Schematic 1. The corresponding BOM values (BOM_Q) were calculated according to previous studies, the only difference was the choice of cutoff point. In previous studies, when the voltage decreased to 20 mV, voltage acquisition was stopped. In this study, the point of maximum voltage drop rate ($Max|\Delta Q/\Delta t|$) was regarded as the cutoff point for voltage acquisition. P-CY is given by formula (1).

$$Q_1 = \int_0^{t_1} Idt = \int_o^{t_1} \frac{U}{R_{ext}} dt \tag{1}$$

where U is the output voltage, R_{ext} is the external resistance, and t_1 is testing time by P-CY.

For easier comparison, P-CY is converted into oxygen consumption (BOM'_Q). Eq. (1) can be rewritten as

$$BOM'_Q = \frac{8000}{FV_{An}} \int_0^{t_1} \frac{U}{R_{ext}} dt (mgO_2L^{-1}) \tag{2}$$

where V_{An} is the effective volume of anolyte (unit: L).

2.3. Electrochemical analyses

Power density and polarization curves are obtained by measuring the voltage over a range of resistance (10000 to 10 Ω) when the MFC reaches a steady state [14]. The coulombic efficiency (CE) is given by formula (3).

$$CE = \frac{C_r}{C_t} \times 100\% \tag{3}$$

where C_r is the real coulomb yield; C_t is the theoretical coulomb yield that can be calculated by△COD (the difference in the influent and effluent chemical oxygen demand) as described previously [15].

The internal resistance of the MFC is obtained by electrochemical impedance spectroscopy (EIS); measurements are taken from 100 kHz to 10 mHz with a sine wave of 10 mV rms (PAR 2273 workstation). The cyclic voltammetry (CV) of the anode is measured over the range of −0.6 V to +0.2 V vs. Ag/AgCl at a scan rate

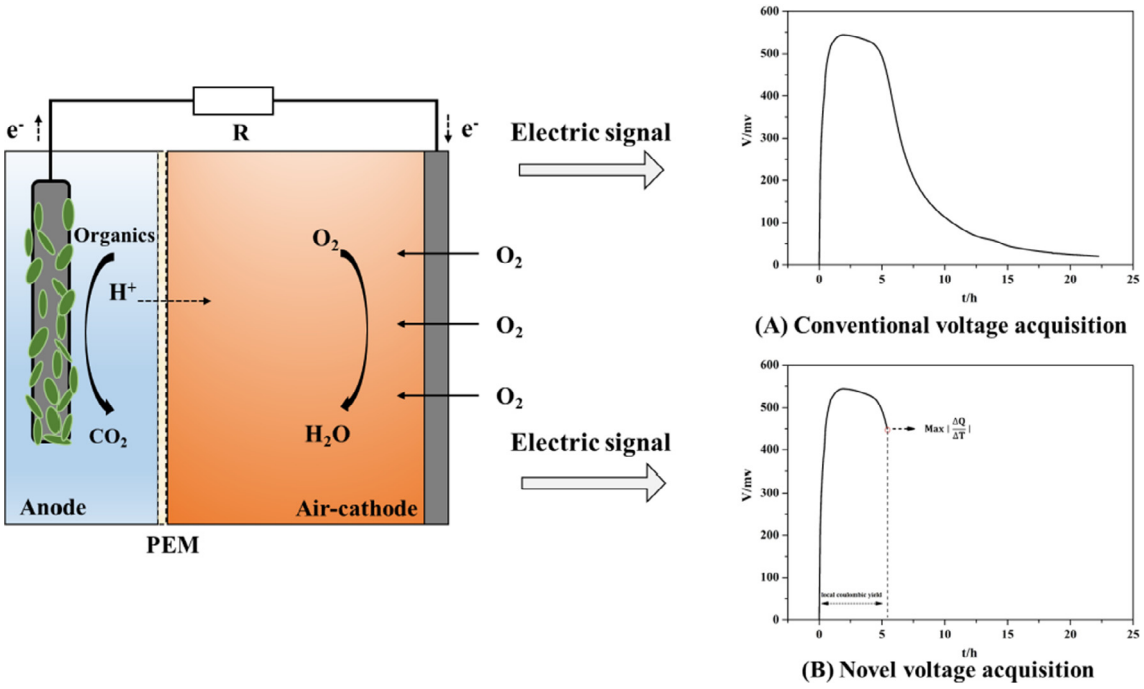

Scheme 1. Illustration of BOM detection in water based on the MFC sensor.

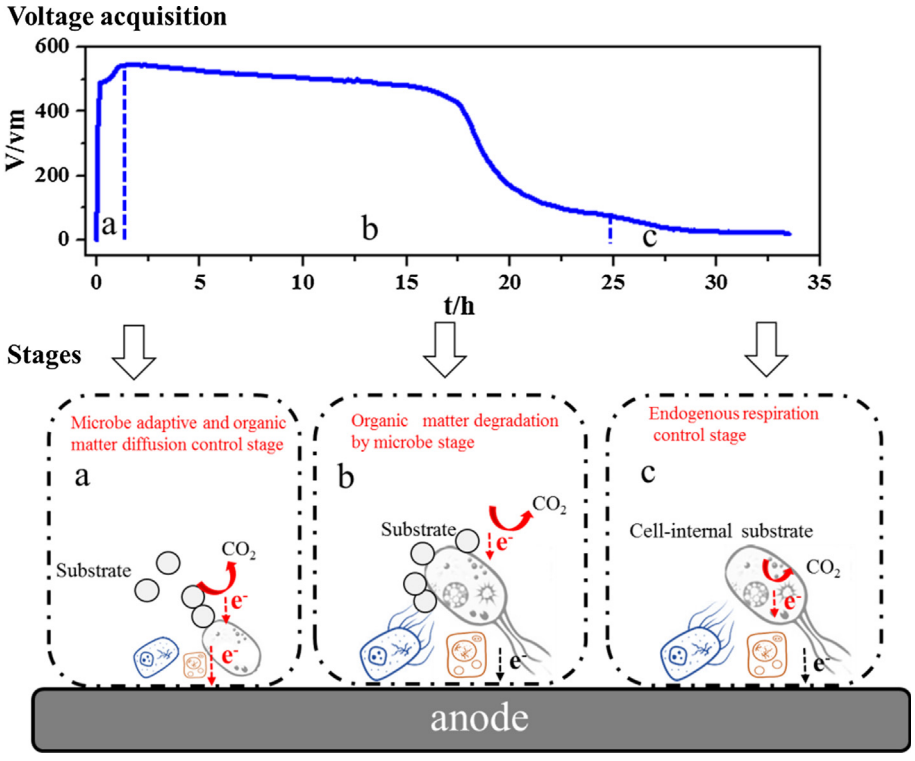

Scheme 2. Diagram of the BOM degradation process by the MFC.

of 50 mV s^{-1} with a CHI660D workstation. COD is measured according to standard methods [16].

2.4. Microbial morphology analysis

The morphology and structure characterizations of the anode biofilms are obtained with a scanning electron microscope (JSM-6510LV, JEOL Co., Ltd., Japan).

3. Results and discussion

3.1. Start-up and performance of the MFC sensor

The voltage output of the MFC sensor during the start-up process is shown in Fig. 1a. The start-up process was performed in a batch mode. As the cycles increased, the voltage gradually increased. It took approximately 5 days to build a biofilm and

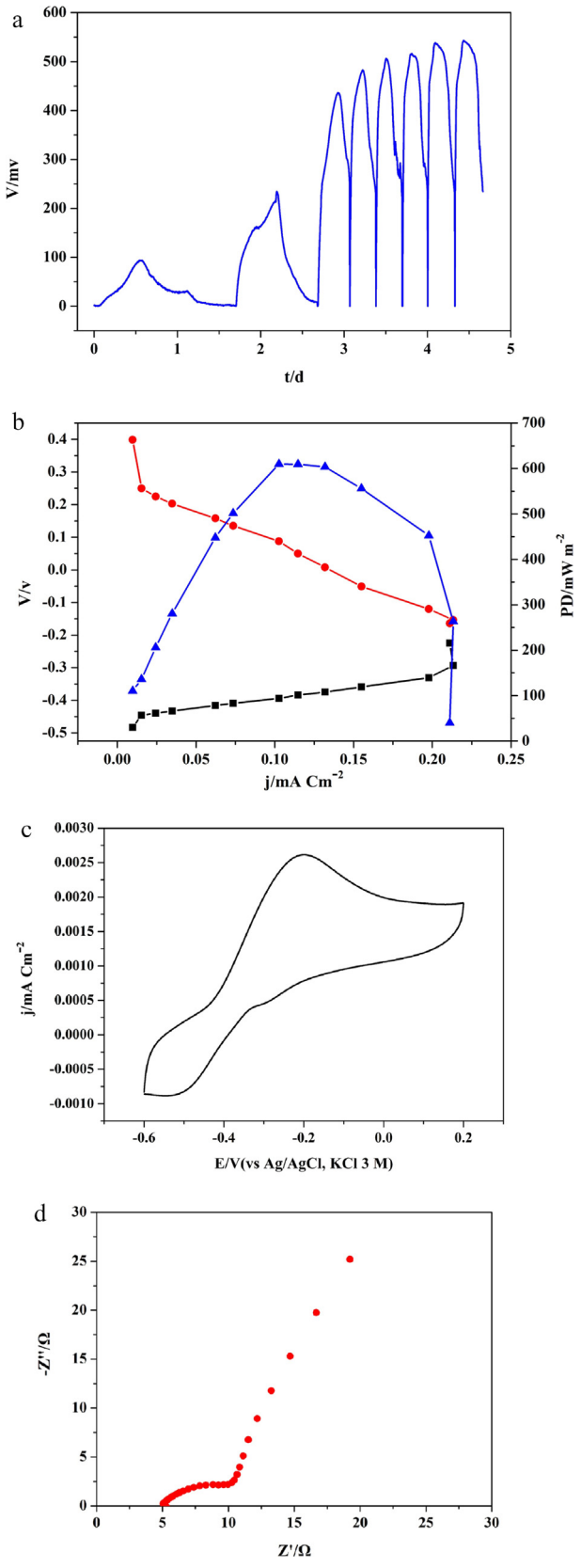

Fig. 1. (a) Voltage output during the start-up process; (b) Power density curve and electrode potentials (Power density, Anode potentials, Cathode potentials); (c) CV curve of the anode; (d) Nyquist plot of the anode.

achieve a stable voltage output [1]. Fig. 1b shows the power density curve and electrode potentials of the stable MFC sensor. The maximum power density was 609.84 mW m^{-2}, the anode potential at the open circuit was −0.483 V (vs. Ag/AgCl). The cathodic potential at the open circuit was 0.399 V (vs. Ag/AgCl). CV curve of the MFC anode tested in a standard GGA solution at a scan rate of 0.05 V/s can be seen in Fig. 1c. A redox peak was observed over the range of −0.21~−0.187 V, which was similar to previous study [17]. EIS was tested and fitted with an equivalent circuit model (constant phase model, CPE) according to the previous study [18]. The Nyquist plot of the anode is shown in Fig. 1d, and the Nyquist plots of the cathode and MFC are shown in Fig. S1 and Fig. S2, respectively. The ohmic resistance (R_{ohm}) and charge-transfer resistance (R_{ct}) of the MFC sensor are listed in Table 1. Fig. 2a and b show SEM images of carbon cloths before and after start-up; the SEM images show that the membrane-hanging was very successful.

3.2. Accuracy and sensitivity of P-CY for BOM measurements

The GGA samples are tested by the MFC sensor, voltage acquisition curves and the voltage drop rate curves are shown in Fig. 3. When the concentration of the GGA samples was greater than or equal to 37.5 mg L^{-1}, there was an apparent peak value on the voltage drop rate curve. However, when the concentration of the GGA samples was below 37.5 mg L^{-1}, it was difficult to identify the peak value. This may be the drawback of this method, but these results clearly show that the detection of BOM at low and high concentrations has involved different dynamic processes. A possible reason for these results is that endogenous respiration is the main factor impacting the voltage drop in low concentration wastewater detection, but by contrast, the sample concentration is the main factor that impacts the voltage drop in high concentration wastewater detection.

Fig. 4 presents the different regression coefficients (R^2) for BOM and the concentrations of GGA samples with CY and P-CY. It was clear that the correlation became more linear (R^2 of 0.999) when P-CY was used, which meant that the new method was more effective compared with conventional coulombic yield when the concentration of the GGA samples was greater than 37.5 mg L^{-1}. Moreover, the linear regression of the data obtained from P-CY was y = 1.11x − 32.85, and the horizontal intercept was 29.59, which also revealed that there were different reaction kinetics for degradation of high concentration and low concentration organics in the MFC sensor. The sensitivity of the MFC sensor can be determined by the difference of the coulombic yield when concentrations of BOM changes. Because of the decreasing coulombic acquisition, the sensitivity of P-CY was slightly lower than CY, but this had no effect on the feasibility of this method.

3.3. Response time and stability of P-CY for BOM measurements

The response time of the two approaches is shown in Fig. 5. The response time of P-CY is shorter than CY, especially at lower substrate concentrations; when the concentration of the GGA samples

Table 1
Simulated values of the resistance (R) of the equivalent circuit.

	R_{ohm} (Ω)	R_{ct} (Ω)
MFC	41.15 ± 0.27	8.43 ± 1.03
Anode	5.14 ± 0.09	2.59 ± 0.25
Cathode	14.60 ± 0.36	3.19 ± 0.76

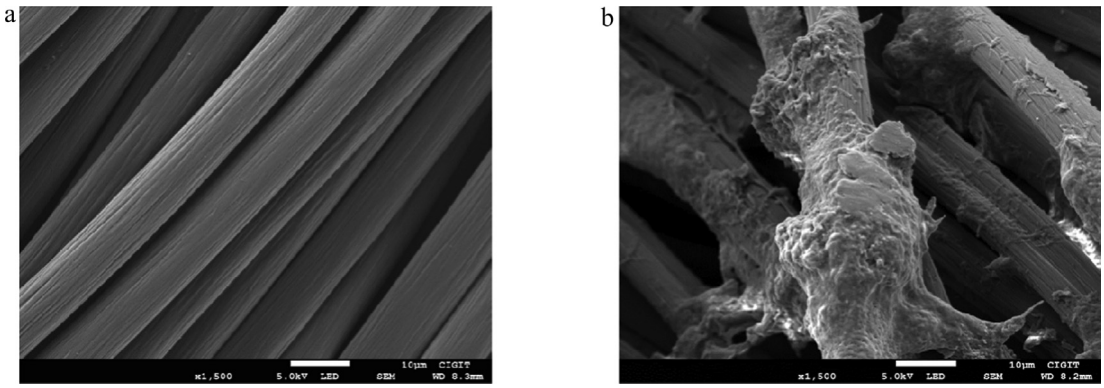

Fig. 2. SEM images of (a) carbon cloth; (b) biofilms attached to the carbon cloth.

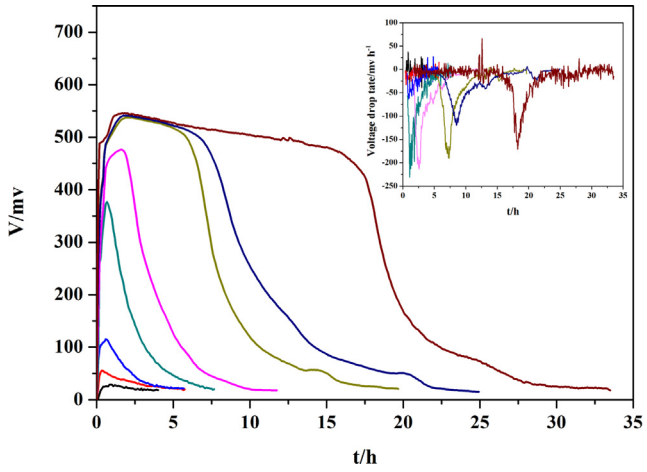

Fig. 3. Cell voltage output of GGA solution samples with different concentrations, pH of 7.0, 30 ± 1 °C (— 3.75 mg L^{-1}, — 7.5 mg L^{-1}, — 15 mg L^{-1}, — 37.5 mg L^{-1}, - - 75 mg L^{-1}, — 150 mg L^{-1}, — 225 mg L^{-1}, — 375 mg L^{-1}).

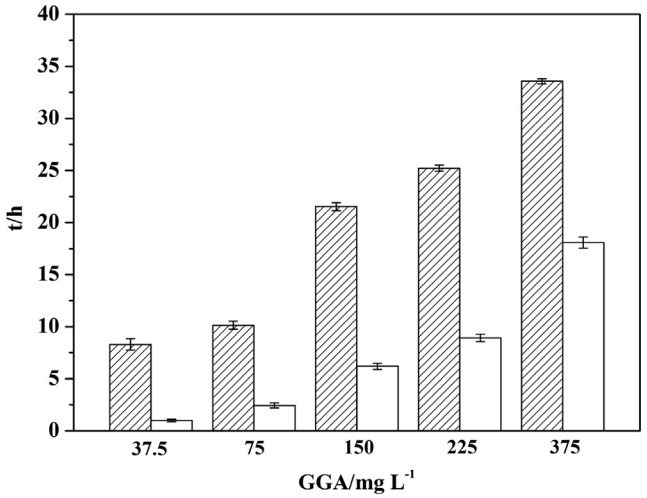

Fig. 5. Response time of CY and P-CY at different concentration of BOM (▨ CY, □ P-CY).

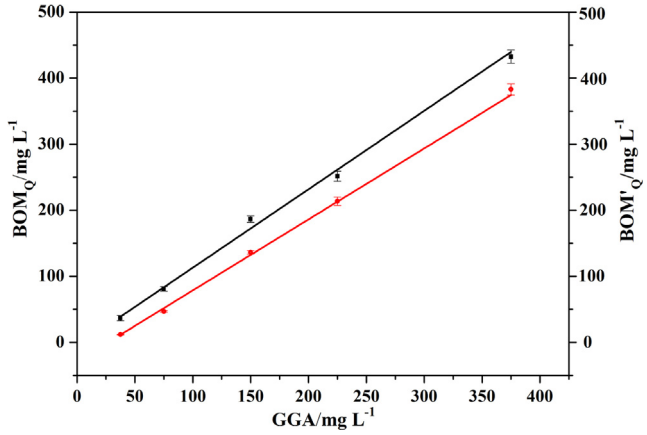

Fig. 4. Linear regression of the data obtained from CY (y = 1.16x-3.03, R^2 = 0.9968) and P-CY (y = 1.11x-32.85, R^2 = 0.9996), BOM_Q was the BOM value calculated by CY, BOM'_Q was the BOM value calculated by P-CY (— CY, — P-CY).

was 37.5 mg L^{-1}, the response time of P-CY was only 0.99 ± 0.18 h, while the response time of CY was 8.29 ± 0.54 h.

The BOM'_Q and BOM_Q values obtained by the MFC sensor are listed in Table 2. The RSD values of the BOM'_Q of the samples varied from ±1.99% to ±3.91%, while those of BOM_Q varied from ±2.31% to ±11.31%. The data indicate that P-CY outperformed CY with respect to stability, the most likely reason for this is that voltage acquisition at the tail stage became less stable, as influence of endogenous respiration.

3.4. Electrochemical performance of the cutoff point of voltage acquisition

The performance of the anode is the key factor of the MFC sensor [18]. Table 3 compares anode EIS behavior with respect to the cutoff point for CY and P-CY. The associated R_{ohm} and R_{ct} values for the cutoff point for P-CY ranged from 6.33 ± 0.01 Ω to 7.77 ± 2.20 Ω and 4.32 ± 0.10 Ω to 8.63 ± 2.00 Ω, with respect to the cutoff point for CY. The fluctuation of the associated R_{ohm} and R_{ct} changed strongly, ranging from 5.08 ± 0.00 Ω to 9.35 ± 0.00 Ω and 4.47 ± 0. 10 Ω to 17.50 ± 0.31 Ω, which indirectly demonstrated that P-CY was more stable than CY. Meanwhile, the R_{ct} of the anode decreased with increasing GGA concentration and appeared to rebound when the concentration of the GGA samples was 375 mg L^{-1} as a high concentration substrate generated more microbial biomass on the anode than a low concentration substrate. Stronger microbial activity induces a reduction in anode internal resistance. Higher substrate concentrations, however, may have some side effects, such as methanogen growth, which is not beneficial to the growth of electricigen [9,19].

Table 2
Stability of BOM'_Q and BOM_Q measurements with the MFC sensor.

GGA concentrations (mg L^{-1})	Theoretical BOD_5 value (mg L^{-1})	BOM_Q (mg L^{-1})	RSD_1 (±%, n = 3)	BOM'_Q (mg L^{-1})	RSD_2 (±%, n = 3)
37.5	50	36.7 ± 4.2	11.3%	11.9 ± 0.5	3.9%
75	100	80.8 ± 3.6	4.4%	46.8 ± 1.4	2.9%
150	200	186.7 ± 5.0	2.7%	136.3 ± 2.7	2.0%
225	300	251.7 ± 7.5	3.0%	213.7 ± 6.5	3.0%
375	500	432.5 ± 10.0	2.3%	383.0 ± 8.6	2.3%

Note: RSD_1 is the relative standard deviation of BOM_Q, RSD_2 is the relative standard deviation of BOM'_Q.

Table 3
Anode EIS behavior at the cutoff point for CY and P-CY.

GGA concentrations (mg L^{-1})	P-CY EIS test (average values)		CY EIS test (average values)	
	R_{ohm} (Ω)	R_{ct} (Ω)	R_{ohm} (Ω)	R_{ct} (Ω)
37.5	6.83 ± 0.34	8.63 ± 2.00	5.08 ± 0.00	17.50 ± 0.31
75	6.33 ± 0.01	6.28 ± 0.16	6.32 ± 0.11	9.31 ± 0.63
150	6.37 ± 0.15	5.97 ± 0.66	7.32 ± 0.84	7.87 ± 1.45
225	7.17 ± 0.00	4.32 ± 0.10	9.35 ± 0.00	4.47 ± 0.10
375	7.77 ± 2.20	6.35 ± 0.41	9.27 ± 0.92	6.21 ± 1.99

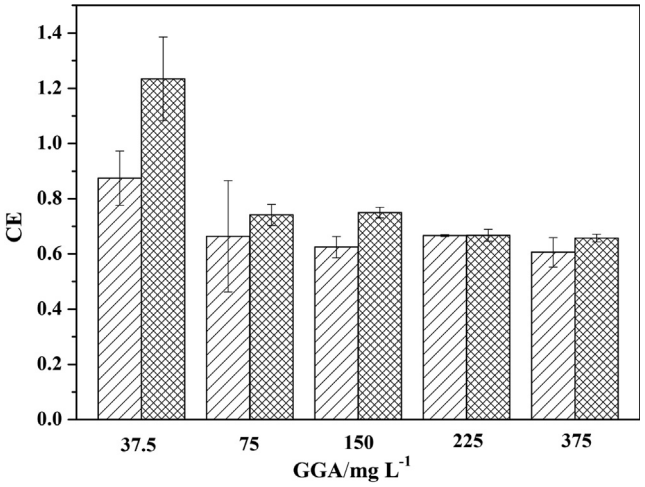

Fig. 6. Coulomb efficiency (CE) of P-CY and CY (▨ P-CY, ▩ CY).

CE is a significant index for evaluating the efficiency of the bioelectrochemical system [9]. The biggest challenge for the CY method lies in maintaining a constant CE when the BOM concentration changes [12]. The CE of the P-CY and CY is shown in Fig. 6. The CE of the P-CY remained more stable than that of the CY, particularly in the detection of low concentrations of GGA. The provision of extra electrons in the tail stage through endogenous respiration most likely explains the high CE values.

3.5. Dynamic model of the cutoff point of voltage acquisition

The MFC sensor is sensitive to microbial species, endogenous respiration, environmental factors, the concentrations and types sorts of the organic compounds, etc [9,20–22]. It is difficult to study the kinetics involved in the relationship between the rate of current (or voltage) change and the organic concentration in the MFC sensors. In this study, all of the interference factors mentioned were controlled at the start-up stage except for the organic concentration. The process of electricity generation can be preliminarily divided into three stages: (1) the microbe adaptive and the chemical diffusion control stage, (2) microbe degrading organic matter stage, and (3) endogenous respiration control stage, as illustrated in Schematic 2.

At stage I, microbes gradually adapt to the new ambient and organics gradually diffuse to the surface of biofilms, and either of these can limit the rate of current increase. At stage III, endogenous respiration is the main factor for the rate of current increase and provide extra electrons at the tail stage.

At stage II, microbes exhibit higher activity stability. The reaction system for BOM degradation is supposed to be in equilibrium; thus, the voltage (current) output represents the BOM degradation reaction velocity. The derivative of s with respect to time (t) is equal to the BOM degradation reaction velocity; the relationship is written as formula (4).

$$U = a\frac{ds}{dt} \tag{4}$$

where s is the real-time BOM concentration; a is the degradation constant; U is the output voltage caused by the organic concentration.

The relationship between voltage output and BOM concentration is obtained from the *Michaelis-Menten* Equation. This relationship is given by formula (5).

$$U = U_{\max}\frac{s}{b+s} \tag{5}$$

where U is the output voltage caused by the organic concentration, s; U_{max} is the maximum voltage output; b is a constant.

From formulas (4) and (5), the relationship between U and t is calculated as:

$$t = \frac{abIn(\frac{bU}{U_{\max}-U}) + \frac{abU}{U_{\max}-U}}{U_{\max}} + C \tag{6}$$

In the initial tests, t = 0; s = s_0. With these values entering into equation (6), the equation can be rewritten as

$$t = \frac{abIn(\frac{bU}{U_{\max}-U}) + \frac{abU}{U_{\max}-U}}{U_{\max}} - \frac{abIns_0 + as_0}{U_{\max}} \tag{7}$$

The derivative of U with respect to t is calculated as:

$$V = \frac{dU}{dt} = \frac{-U(U_{\max}-U)^2}{abU_{\max}} \tag{8}$$

where V is the voltage drop rate.

The second derivative of U with respect to t is calculated as:

$$\frac{dV}{dt} = \frac{d^2U}{dt^2} = \frac{U(U_{\max}-3U)(U-U_{\max})^3}{a^2b^2U_{\max}^2} \quad (0 \leqslant U \leqslant Umax) \tag{9}$$

Table 4
BOM measurements of different real wastewaters.

Samples	BOD_5 (mg L^{-1})	BOM_Q (mg L^{-1})	T_1(h)	BOM'_Q (mg L^{-1})	T_2(h)
Municipal wastewater-1	11.2 ± 1.0	–	–	–	–
Municipal wastewater-2	91.6 ± 3.2	38.8 ± 0.7	15.19 ± 2.63	–	–
Municipal wastewater-3	254.7 ± 3.1	138.5 ± 1.9	12.94 ± 1.57	108.9 ± 3.7	5.47 ± 0.41
Municipal wastewater-4	193.7 ± 12.8	129.5 ± 6.7	22.64 ± 2.34	80.9 ± 15.3	5.28 ± 1.21
Pharmaceutical wastewater	1454.7 ± 140.2	949.4 ± 28.5	20.83 ± 2.00	833.4 ± 30.7	11.22 ± 0.47
Beer industry wastewater	274.5 ± 13.7	244.9 ± 5.1	19.31 ± 1.76	238.4 ± 10.7	17.53 ± 4.52

Note: T_1 is the response time of CY for the diluted samples, T_2 is the response time of P-CY for the diluted samples, "-" means the result is not available.

When $Umax/3 \leq U \leq Umax$, $dV/dt > 0$, V increases as a function of time; when $0 \leq U \leq Umax/3$, $dV/dt < 0$, V decreases with time, and $V < 0$. Therefore, with a voltage decreasing, there should be an inflection point where a maximum voltage drop rate is reached, and the voltage value of the inflection point is Umax/3. This study indirectly proves that the point of the maximum rate of voltage drop is in stage II. Adopting this point as the cutoff point can prevent the severe deviation at stage III and shorten the testing time. It is noticeable, however, that the measured voltage value of the inflection point is not equal to the theoretical voltage value because of the interference from reaction products and enzyme utilization.

3.6. BOM measurements of different real wastewaters

Results of BOM measurements for different real wastewaters are listed in Table 4. It is obvious that P-CY took less time (T_2) than CY (T_1), in addition, the corresponding BOM'_Q values have good stability. This method is testified to be applicable in practice. The wastewater samples of municipal wastewater-1 and municipal wastewater-2 cannot be measured by P-CY as the BOM concentration is below its detection limit. This result is consistent with that of artificial wastewater. In addition, the BOM_Q values are significantly less than BOD_5 values. This may also be explained that the complex substrates are difficult to detect using MFC sensors [9], and that large amount of NO_3^- in water samples consumes the electrons released from the organic matter [10]. Thus, the BOM measurements of the complex wastewater needs to be further explored.

4. Conclusion

This study presented a new calculation method (P-CY) for accelerating the BOM measurements by using MFC sensor in which P-CY was applied to higher concentrations of BOM (37.5–375 mg L^{-1}). Compared to CY, P-CY performed much higher accuracy (R^2 of 0.999) and relatively shorter response time (0.99 ± 0.18–18.08 ± 0.58 h). Electrochemical tests were also carried out to investigate the cutoff points for CY and P-CY. The results showed that the electrochemical characteristics of the cutoff point for P-CY were more stable, resulting in measurements of higher precision. Moreover, a mathematical model was established to verify the rationality of the cutoff point for P-CY, which revealed that during the voltage drop, there must be an inflection point where a maximum voltage drop rate was reached. Furthermore, properly choosing the cutoff point could effectively avoid the effects of product accumulation and endogenous respiration occurring in the tail stage.

Declaration of Competing Interest

The authors declare that they have no known competing financial interests or personal relationships that could have appeared to influence the work reported in this paper.

Acknowledgments

This work was supported by the National Natural Science Foundation of China (51525805, 51727812 and 51808526) and the Natural Science Foundation of Chongqing (No. cstc2018jcyjAX0327).

Appendix A. Supplementary data

Supplementary data to this article can be found online at https://doi.org/10.1016/j.bioelechem.2020.107488.

References

[1] Y. Liu, A.X. Tuo, X.J. Jin, X.Z. Li, H. Liu, Quantifying biodegradable organic matter in polluted water on the basis of coulombic yield, Talanta 176 (2018) 485–491, https://doi.org/10.1016/j.talanta.2017.08.029.
[2] S. Jouanneau, L. Recoules, M.J. Durand, A. Boukabache, V. Picot, Y. Primault, A. Lakel, M. Sengelin, B. Barillon, G. Thouand, Methods for assessing biochemical oxygen demand (BOD): a review, Water Res. 49 (2014) 62–82, https://doi.org/10.1016/j.watres.2013.10.066.
[3] S.A. Chiappini, D.J. Kormes, M.C. Bonetto, N. Sacco, E. Corton, A new microbial biosensor for organic water pollution based on measurement of carbon dioxide production, Sensors and Actuators B-Chemical 148 (2010) 103–109, https://doi.org/10.1016/j.snb.2010.04.039.
[4] C. Liu, H. Zhao, S. Gao, J. Jia, L. Zhao, D. Yong, S. Dong, A reagent-free tubular biofilm reactor for on-line determination of biochemical oxygen demand, Biosens. Bioelectron. 45 (2013) 213–218, https://doi.org/10.1016/j.bios.2013.01.041.
[5] M. Kim, M.S. Hyun, G.M. Gadd, G.T. Kim, S.J. Lee, H.J. Kim, Membrane-electrode assembly enhances performance of a microbial fuel cell type biological oxygen demand sensor, Environ. Technol. 30 (2009) 329–336, https://doi.org/10.1080/09593330902732077.
[6] J. Liu, B. Mattiasson, Microbial BOD sensors for wastewater analysis, Water Res. 36 (2002) 3786–3802, https://doi.org/10.1016/s0043-1354(02)00101-x.
[7] S. Zhou, S. Huang, Y. Li, N. Zhao, H. Li, I. Angelidaki, Y. Zhang, Microbial fuel cell-based biosensor for toxic carbon monoxide monitoring, Talanta 186 (2018) 368–371, https://doi.org/10.1016/j.talanta.2018.04.084.
[8] H. Jia, W. Liu, J. Wang, H.H. Ngo, W. Guo, H. Zhang, Optimization of sensing performance in an integrated dual sensors system combining microbial fuel cells and upflow anaerobic sludge bed reactor, Chemosphere 210 (2018) 931–940, https://doi.org/10.1016/j.chemosphere.2018.07.119.
[9] M.C. Hsieh, C.Y. Cheng, M.H. Liu, Y.C. Chung, Effects of Operating Parameters on Measurements of Biochemical Oxygen Demand Using a Mediatorless Microbial Fuel Cell, Biosensor. *Sensors (Basel)* 16 (2015), https://doi.org/10.3390/s16010035.
[10] D. Wang, P. Liang, Y. Jiang, P. Liu, B. Miao, W. Hao, X. Huang, Open external circuit for microbial fuel cell sensor to monitor the nitrate in aquatic environment, Biosens. Bioelectron. 111 (2018) 97–101, https://doi.org/10.1016/j.bios.2018.04.018.
[11] M. Kim, S.M. Youn, S.H. Shin, J.G. Jang, S.H. Han, M.S. Hyun, G.M. Gadd, H.J. Kim, Practical field application of a novel BOD monitoring system, J. Environ. Monit. 5 (2003) 640–643, https://doi.org/10.1039/b304583h.
[12] Y. Jiang, X.F. Yang, P. Liang, P.P. Liu, X. Huang, Microbial fuel cell sensors for water quality early warning systems: fundamentals, signal resolution, optimization and future challenges, Renew. Sustain. Energy Rev. 81 (2018) 292–305, https://doi.org/10.1016/j.rser.2017.06.099.
[13] X.H. Zhou, M.K. Zhang, T. Yu, Y.C. Liu, H.C. Shi, Oxygen profiles in biofilms undergoing endogenous respiration, Chem. Eng. J. 220 (2013) 452–458, https://doi.org/10.1016/j.cej.2013.01.004.
[14] X.J. Jin, F. Guo, W.Q. Ma, Y. Liu, H. Liu, Heterotrophic anodic denitrification improves carbon removal and electricity recovery efficiency in microbial fuel cells, Chem. Eng. J. 370 (2019) 527–535, https://doi.org/10.1016/j.cej.2019.03.023.
[15] J.Y. Nam, H.W. Kim, K.H. Lim, H.S. Shin, Effects of organic loading rates on the continuous electricity generation from fermented wastewater using a single-chamber microbial fuel cell, Bioresour. Technol. 101 (Suppl 1) (2010) S33–37, https://doi.org/10.1016/j.biortech.2009.03.062.

[16] G.S. Jadhav, M.M. Ghangrekar, Performance of microbial fuel cell subjected to variation in pH, temperature, external load and substrate concentration, Bioresour. Technol. 100 (2009) 717–723, https://doi.org/10.1016/j.biortech.2008.07.041.
[17] D. Yu, L. Bai, J. Zhai, Y. Wang, S. Dong, Toxicity detection in water containing heavy metal ions with a self-powered microbial fuel cell-based biosensor, Talanta 168 (2017) 210–216, https://doi.org/10.1016/j.talanta.2017.03.048.
[18] T. Gonzalez, M.S. Ureta-Zanartu, J.F. Marco, G. Vidal, Effect of Zeolite-Fe on graphite anode in electroactive biofilm development for application in microbial fuel cells, Appl. Surf. Sci. 467 (2019) 851–859, https://doi.org/10.1016/j.apsusc.2018.10.120.
[19] R.P. Pinto, B. Srinivasan, M.F. Manuel, B. Tartakovsky, A two-population bio-electrochemical model of a microbial fuel cell, Bioresour. Technol. 101 (2010) 5256–5265, https://doi.org/10.1016/j.biortech.2010.01.122.
[20] E.S. Heidrich, J. Dolfing, M.J. Wade, W.T. Sloan, C. Quince, T.P. Curtis, Temperature, inocula and substrate: contrasting electroactive consortia, diversity and performance in microbial fuel cells, Bioelectrochemistry 119 (2018) 43–50, https://doi.org/10.1016/j.bioelechem.2017.07.006.
[21] T.H. Sleutels, L. Darus, H.V. Hamelers, C.J. Buisman, Effect of operational parameters on Coulombic efficiency in bioelectrochemical systems, Bioresour. Technol. 102 (2011) 11172–11176, https://doi.org/10.1016/j.biortech.2011.09.078.
[22] H.S. Lee, P. Parameswaran, A. Kato-Marcus, C.I. Torres, B.E. Rittmann, Evaluation of energy-conversion efficiencies in microbial fuel cells (MFCs) utilizing fermentable and non-fermentable substrates, Water Res. 42 (2008) 1501–1510, https://doi.org/10.1016/j.watres.2007.10.036.